Title	Characteristics of a tsunamigenic megasplay fault in the Nankai Trough
Author(s)	Yamada, Yasuhiro; Masui, Reona; Tsuji, Takeshi
Citation	Geophysical Research Letters (2013), 40(17): 4594-4598
Issue Date	2013-09
URL	http://hdl.handle.net/2433/180091
Right	© 2013. American Geophysical Union.; This is an OnlineOpen article.
Type	Journal Article
Textversion	publisher

Characteristics of a tsunamigenic megasplay fault in the Nankai Trough

Yasuhiro Yamada,[1] Reona Masui,[1] and Takeshi Tsuji[1,2]

Received 27 July 2013; accepted 20 August 2013; published 9 September 2013.

[1] Slip on the shallow part of a megasplay fault that is an out-of-sequence thrust and branch of the main subduction plate boundary can cause devastating tsunamis after earthquakes. We analyzed the three-dimensional geometry, including dip amount and azimuths, roughness distributions, and thickness variations, of the shallow part of a megasplay fault in the Nankai Trough using a three-dimensional seismic data set. The fault is divided into three zones based on its geometry: thick, smooth, and simply convex in the east; complexly curved in the middle; and thin and kinked in the west. Results of scientific drilling indicate that the eastern region of the fault is most active, and local heterogeneities in fault geometry, including roughness and thickness, may control the slip on this part of the fault. The present findings can be used to evaluate the risk of future tsunamis arising from movement on shallow thrust faults at subduction margins. **Citation:** Yamada, Y., R. Masui, and T. Tsuji (2013), Characteristics of a tsunamigenic megasplay fault in the Nankai Trough, *Geophys. Res. Lett.*, *40*, 4594–4598, doi:10.1002/grl.50888.

1. Introduction

[2] Great earthquakes with moment magnitudes of >8.0 take place along plate subduction zones when a megathrust ruptures over a large area, and the associated fault displacements of the ocean floor can generate tsunamis. Examples include the 2004 Sumatra [e.g., *Waldhauser et al*., 2012], 2006 Java [e.g., *Ammon et al*., 2006], and 2011 Tohoku earthquakes [e.g., *Ito et al*., 2011]. Previous studies have speculated that coseismic slip along out-of-sequence thrusts (OOSTs) [*Morley*, 1988] in accretionary prisms may contribute to tsunami generation [*Moore et al*., 2007]. Understanding the nucleation and development of OOSTs is important when studying the structural evolution of accretionary prisms and thrust belts [*Morley*, 1988; *Kao and Chen*, 2000; *Nieuwland et al*., 2000; *Park et al*., 2000; *Mukoyoshi et al*., 2006; *Bangs et al*., 2009].

[3] In the Nankai Trough, the Philippine Sea Plate is being subducted beneath southwest Japan at a rate of 4.0 to 6.5 cm/yr along azimuths of 300° to 315° [*Seno et al*., 1993; *Miyazaki and Heki*, 2001]. Detailed seismic reflection imaging [*Moore et al*., 2007] and scientific ocean drilling [*Kinoshita et al*., 2009] have characterized the accretionary wedge in the Kumano area (Figure 1) and revealed that slip on a large-scale OOST, referred to as a "megasplay" [*Tobin and Kinoshita*, 2006], may periodically cause great earthquakes and associated tsunamis [*Moore et al*., 2007]. The megasplay fault originated as a frontal thrust and functioned as an imbricate thrust system until 1.95 Ma, after which the fault became an out-of-sequence (splay) fault [*Strasser et al*., 2009]. Analyses of shallow slope sediments recovered by drilling ~20 km landward of the trench to the south of Kii Peninsula, where the megasplay intersects the ocean floor, have confirmed that seismic vibrations generated by the fault have triggered submarine slides [*Strasser et al*., 2009; *Sakaguchi et al*., 2011].

[4] It is evident from the 2011 Tohoku earthquake that a large displacement of the ocean floor topography generated its devastating tsunami [*Ito et al*., 2011]. *Kawamura et al*. [2012] interpreted this large displacement of the thrust toe as representing submarine slides triggered by the earthquake, and the resultant movement of the ocean floor is particularly prone to generating and enhancing large tsunamis [*Bardet et al*., 2003; *Matsumoto and Tappin*, 2003; *Satake*, 2012]. Therefore, it is prudent to examine the slip potential of the shallow part of the megasplay fault in terms of the risk of generating tsunamis in the Nankai Trough.

[5] Based on topography and the distribution of slope failures on the ocean floor in the Kumano area of the Nankai Trough, activity of the shallow part of the megasplay fault in the past ~1.55 Ma is inferred to have varied along strike, being characterized by relatively active and inactive regions [*Kimura et al*., 2011]. In particular, the eastern domain of this area continued to be active after 1.55 Ma, whereas the western domain ceased activity at 1.55 Ma, forepart from a short period of activity at approximately 1.24 Ma [*Kimura et al*., 2011]. If these local differences are induced by seamount subduction, as suggested by *Kimura et al*. [2011] (Figure 1b), then the geometry of the megasplay fault may also show corresponding lateral differences. Herein, we describe the detailed geometric characteristics of the shallow part of the megasplay fault in the Nankai Trough and examine their relationship to lateral variations in fault activity. Our study uses three-dimensional seismic and scientific drilling data from the plate subduction margin and is the first attempt to reveal the relationship between in situ fault characteristics and their tsunami-generating potential.

2. Methods

[6] We used Integrated Ocean Drilling Program (IODP) data from sites C0004 and C0010 with a three-dimensional reflection seismic data set (three-dimensional prestack depth migration; see *Moore et al*. [2009] for details of the data set) to examine the detailed geometry of the megasplay fault in the Kumano area of the Nankai Trough, including thickness variations of the fault zone (the perpendicular distance between the top and bottom surfaces of the zone) (Figure 1). We also examined the roughness distribution of the fault surface.

[1]Department of Earth Resources Engineering, Kyoto University, Kyoto, Japan.
[2]International Institute for Carbon Neutral Energy Research (WPI-I2CNER), Kyushu University, Fukuoka, Japan.

Corresponding author: Y. Yamada, Graduate School of Engineering, Kyoto University, Katsura, Kyoto 615-8540, Japan. (yamada@earth.kumst.kyoto-u.ac.jp)

0094-8276/13/10.1002/grl.50888

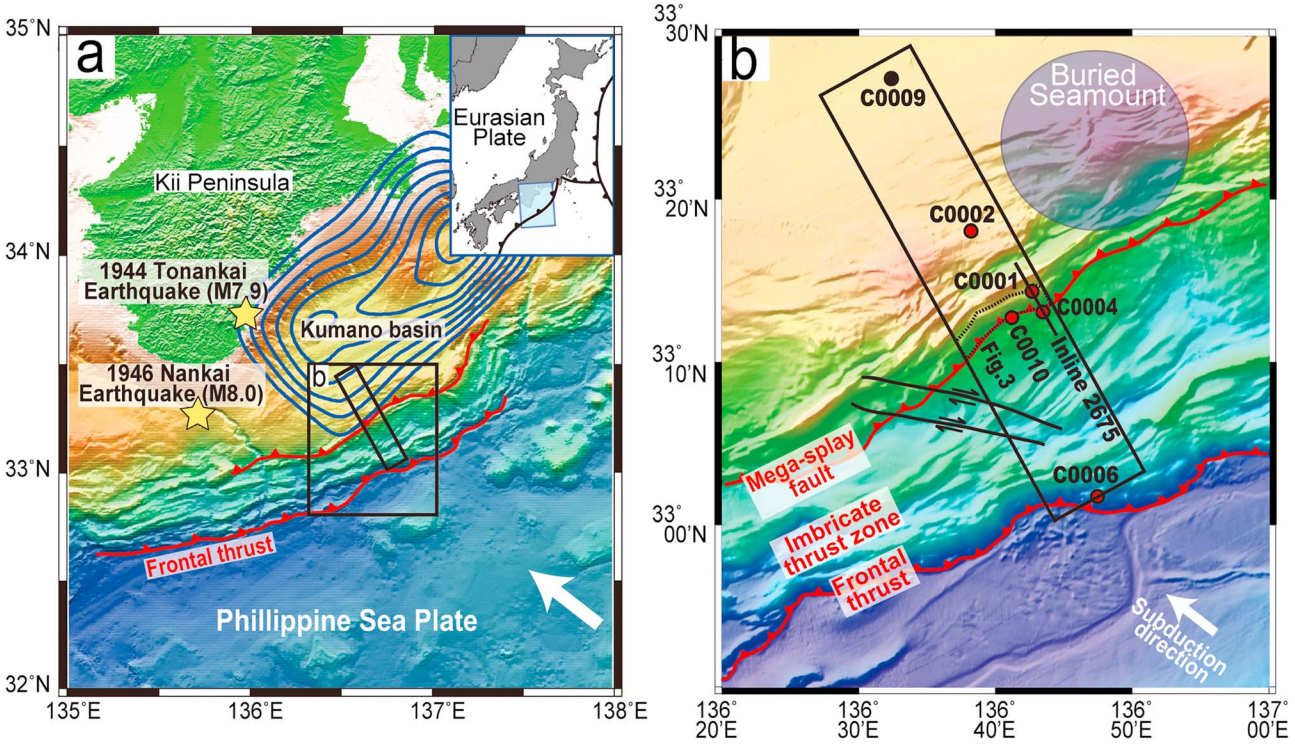

Figure 1. Location map of the study area. (a) Blue contours around the Kumano Basin show the coseismic slip distribution of the 1944 Tonankai earthquake [*Kikuchi et al*., 2003]. (b) C0001–C0009 are the IODP wells of the Nankai Trough Seismogenic Zone Experiment project. The seamount location is based on *Kimura et al*. [2011].

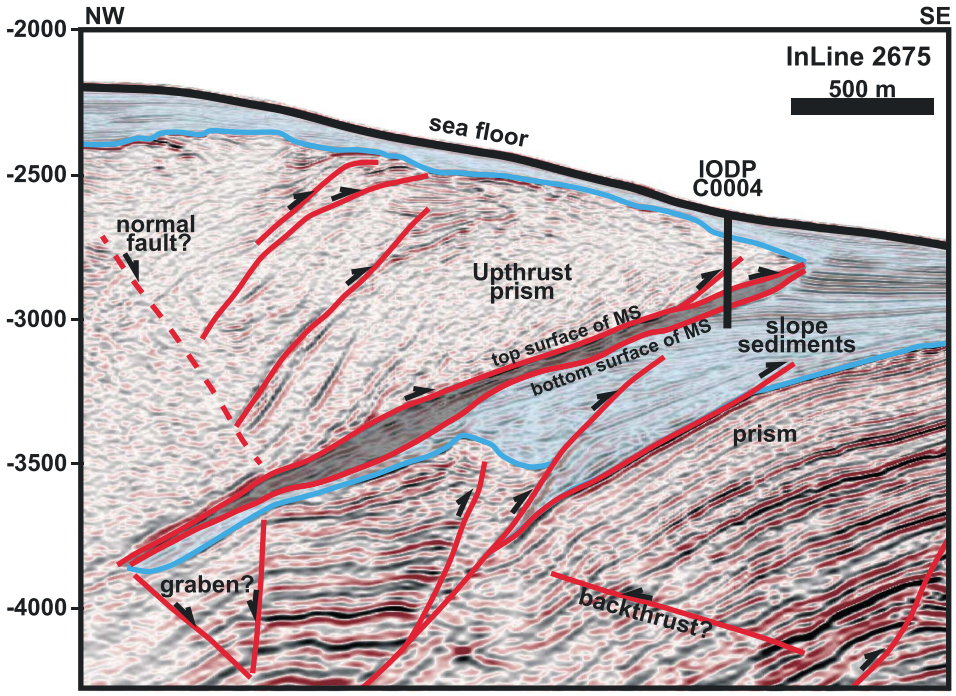

Figure 2. Seismic profile through C0004. The shaded zone bounded by the top and bottom surfaces corresponds to the megasplay fault zone traced from the IODP holes at site C0004. The accretionary prism contains a variety of faults (red) and folds and is covered by slope sediments (blue). The black line is the ocean floor. The geological interpretation of the slope sediments was modified after *Kimura et al*. [2011].

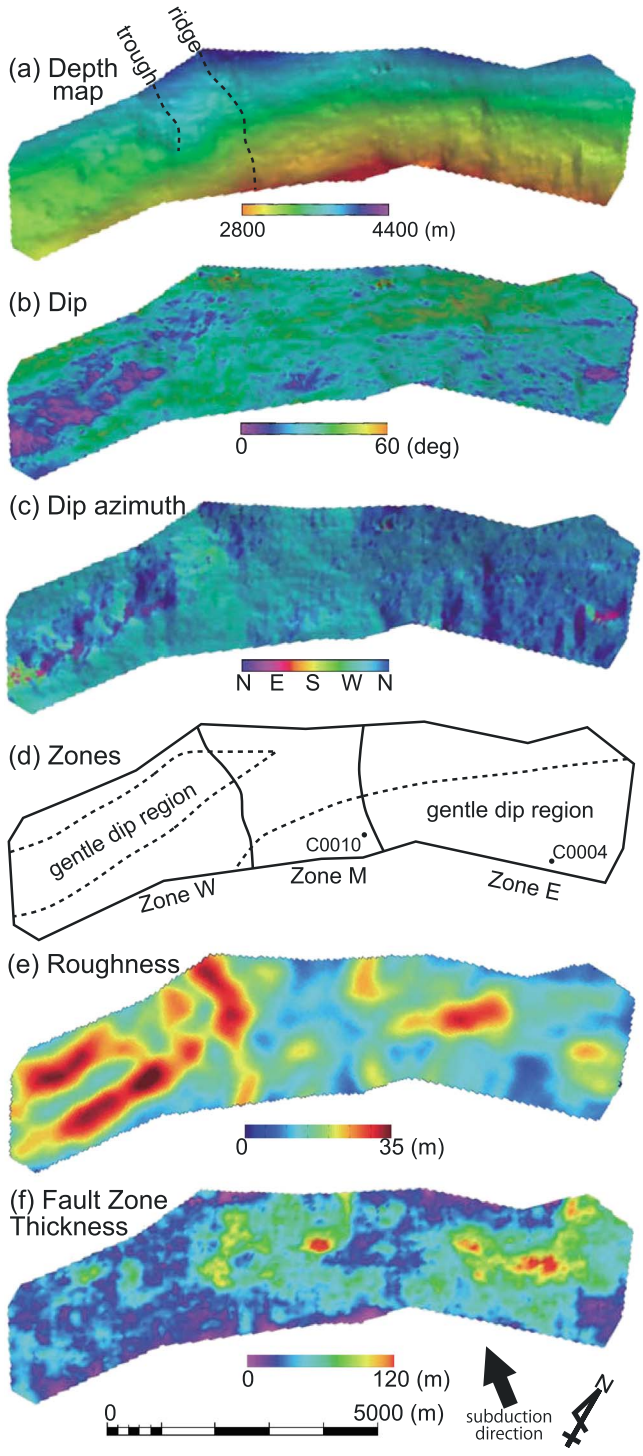

Figure 3. Detailed geometry of the seismogenic megasplay fault zone in the Nankai Trough: (a) depth contours, (b) dip angles, (c) dip azimuths, (d) fault segments based on dip angle, (e) roughness of the top surface of the fault zone, and (f) the thickness of the fault zone. IODP sites C0004 and C0010 are also shown in Figure 3d. The location of this region is indicated in Figure 1. See text for details of the roughness calculations.

[7] The shallow part of the fault has been penetrated several times during IODP drilling, and geophysical logging data and core samples have been recovered from the fault zone. We first examined data from hole C0004B of IODP Expedition 314 (Figures 1 and 2), which showed that the fault consists of inhomogeneous fracture zones ranging in thickness from 45 to 59 m [*Kinoshita et al*., 2009; *Yamada et al*., 2011]. Core samples at site C0004 from IODP Expedition 316 confirm the logging data from C0004B and show that the megasplay fault is characterized by a zone of fractured/brecciated rock with slickensides oriented in a variety of directions [*Kinoshita et al*., 2009]. Site C0010 of IODP Expedition 319 (Figure 1) also penetrated through the megasplay fault at a site 3.5 km along strike of site C0004, but here the fault characteristics are unclear due to the poor quality of the geophysical logging data and lack of core samples [*Saffer et al*., 2010]. We used the C0010 data to constrain the approximate depth of the megasplay fault at this site.

[8] Our interpretation of the megasplay fault from the three-dimensional seismic data set is based on the fault depth at the IODP holes and the distinct reflections produced by the top and bottom surfaces of the fault zone. Where the reflections from these surfaces were weak, we also used truncations of reflections from the footwall and hanging wall. Minor thrusts that branch from the megasplay to the hanging wall were also examined to identify the top surface (e.g., Figure 2). Our study area of the megasplay is spatially defined by the edges of the three-dimensional seismic data set in the northeast and southwest, the tip line of the fault in the southeast, and the deeper limit of continuous reflections of the fault in the northwest.

[9] Estimation of the fault zone thickness from reflection signals is not always possible due to the tuning effect, and fault zones that can be resolved as plural reflections in a seismic profile need to have a vertical scale greater than a quarter of the wavelength [*Sheriff*, 2002]. As shown below, the fault thickness, as defined by the perpendicular distance between the top and bottom surfaces of the fault zone, in the study area generally exceeds this theoretical limit of vertical resolution. This limit of resolution is 5–7 m for near-surface sediments and 10–20 m for the deepest sediments at the study site [*Yamada et al*., 2011]. We also used IODP C0004B well data to correlate reflection signals with the fault interval derived from the logging data [*Yamada et al*., 2011].

[10] To extract further details of the megasplay fault geometry, we calculated the roughness distribution of the top surface of the fault zone based on the root-mean-square (RMS) method. This procedure requires three steps: (1) creation of a grid system at 50 m intervals (base grid) on the surface and extraction of coordinate data from all the grid points; (2) creation of another grid system of any size (target grid) that is larger than the base grid; (3) collation of all base grid points within each target grid and determination of a plane called the "average surface" using the least squares method; (4) calculation of the distance between the base grid points and the average surface using RMS, and using the results of this as the roughness of the target grid; and (5) repeating steps 3 and 4 for all the target grids. The unit of this roughness distribution is in meters, and large values correspond to regions where the fault surface anomalously deviates from the smooth averaged fault surface. The calculated roughness distribution depends on the size of the target grid; consequently, local and regional roughness can be evaluated with small and large grids, respectively.

3. Results

[11] In general, the shallow part of the megasplay fault dips to the NW and has a gentle convex curvature in plan view

(Figure 3a). A contour map of the top surface of the fault shows its shape to be a gentle trough and ridge in the western region and a series of minor crenulations in the eastern region. All of these features trend NNW-SSE (Figure 3a). However, a detailed map of dip angle and azimuth patterns (Figures 3b and 3c) shows that the surface geometry is more complex and three zones can be recognized (Figure 3d). Zone E is characterized by a simple convex-upward geometry, gentle NNW dips, several lineation features in its shallow part, and steeper dips at depth. Zone W generally dips to the NW apart from at intermediate depths where the surface is nearly horizontal (Figure 3b). The boundaries between this horizontal area and the surrounding moderately dipping (30°–40°) areas can be clearly defined. Zone M is located between Zones E and W and has a dip azimuth that gradually changes from west in the eastern area to north in the western area. Given that the dip angle has a sinusoidal pattern, with steeper angles at intermediate depths, the fault surface in Zone M has a complexly curved three-dimensional geometry. In all zones, minor undulations with wavelengths of a few hundreds of meters can also be observed in the dip angle and azimuth patterns (Figures 3b and 3c). The dip azimuth map shows many anomalous dots (artifacts) in Zones E and W that are due to very low dip angles. The geometry of the bottom surface of the megasplay fault zone is almost the same as that of the top surface, apart from subtle differences due to thickness variations of the fault zone.

[12] The roughness distributions of the megasplay fault surface at a grid size of 1050 m (Figure 3e) show two systems of high-roughness anomalies, oriented NW-SE and NE-SW. The NW-SE anomaly corresponds to the boundaries of the three zones, whereas the NE-SW anomaly corresponds to the boundaries of the gentle dip regions. These results suggest that the fault surface in Zone W is kinked, but in Zones E and M, the fault surface is relatively smooth.

[13] The megasplay fault zone is generally 20–40 m thick (Figure 3f), except in regions close to the tip line (southeastern fault edge) where the thickness is zero. The roughness distribution also identifies several areas of the fault zone where it is thicker in Zones E and M, and in these places, the maximum thickness is approximately 120 m. Around the northwestern border of the study area, where the splay fault is deeply buried, the observed thickness variations may not be precise due to the poor quality of the seismic reflection data.

4. Lateral Variations in Fault Zone Characteristics and Their Relationship to Fault Activity

[14] Our analysis of the megasplay fault geometry shows that the fault has three zones with different structural styles. Thrust faults generally change geometry with evolution due to processes such as segment linkage [*Cartwright et al*., 1995; *Walsh et al*., 2003], propagation across barriers [*Ellis and Dunlap*, 1988], and subsequent deformation after fault formation [e.g., *Yamada et al*., 2006; *Miyakawa et al*., 2010]. Fault thickness can also be used to assess the long-term fault activity, since thickness generally increases with displacement [*Hull*, 1988; *Evans*, 1990]. Given that the general tectonic setting and sedimentary sequences are essentially the same throughout the study region, the geometric characteristics identified in our study may be due to different evolutionary histories in the three zones. We now consider the activity of these three zones based on their geometry and deformation processes as constrained by the thickness distributions.

[15] The simple convex geometry of Zone E is commonly observed in natural and model accretionary wedges where a thrust propagates to the wedge surface and displaces the hanging wall over a footwall consisting of younger and porous sediments [e.g., *Yamada et al*., 2006]. As our study focused on the shallow part of the megasplay fault and its footwall comprises younger slope basin deposits [*Strasser et al*., 2009], the identified fault geometry can be assumed to have the shape of a thrust that has not experienced severe subsequent deformation after thrust formation. The simply curved and thickened geometry suggests that this zone has, until recently, been active for a long time. The distribution of the surface slope failure deposits also indicates that Zone E has recently been active.

[16] The kinked geometry of Zone W is indicative of a passive deformation due to the effects of surrounding deformation structures. Such passive deformation of inactive thrusts is commonly observed in modeled accretionary wedges [e.g., *Yamada et al*., 2006; *Miyakawa et al*., 2010]. As such, Zone W may presently be inactive, as also indicated by the scarcity of slope failure deposits associated with this zone. Zone W is thinner than the other zones, which implies that here the fault may have been less active and the displacement smaller than for the other zones. The kinked geometry in Zone W is unclear in the area adjacent to Zone M, where the dip azimuth is rotated slightly to the west (Figure 3c). This suggests that the eastern margin of Zone W has acquired additional external strain, probably from Zone M, and that this strain has deformed this part of Zone W.

[17] Zone M has a complexly curved geometry but is rather smooth and has no kinked features, suggesting that the fault might be active in this zone, as also indicated by submarine slope failures identified from ocean floor topography [*Kimura et al*., 2011]. The obscure boundary with Zone E in the fault roughness map suggests that the megasplay fault displacement in Zone M may be similar to that in Zone E. In contrast, the distinctive boundary between Zones W and M in the fault roughness map (Figure 3e) and their thickness differences (Figure 3f) indicate a possible major gap in fault displacement that should have generated associated deformation structures around the boundary between the zones. The complexly folded geometry of Zone M and the change in dip azimuth in the eastern part of Zone W may have been induced by effects associated with the displacement gap. As proposed by *Ellis and Dunlap* [1988], a thrust fault may bend during its development (segment linkage) where a barrier exists. The kinked geometry of Zone W may have acted as such a barrier and prevented propagation of fault displacement from Zone M. The slight change in the dip azimuth of the megasplay fault from Zone W (NW) to Zone E (NNW) (Figure 3c) and its associated strain may also have contributed to the deformation geometry of Zone M.

[18] Given that the megasplay fault consists of three intensely or moderately fractured zones in Zone E (e.g., C0004B) [*Yamada et al*., 2011], thickening may have proceeded in several stages rather than as a continuous process. *Gulick et al*. [2010] examined lateral thickness variations in the slope sediments (Figure 2) and argued that the megasplay fault may be a transient and short-lived structure and that parts of the fault may have ceased activity. These observations indicate that the geometrical characteristics of the megasplay described here may also develop intermittently and be transient in nature.

[19] Our study has identified that Zone E of the megasplay fault has a thickened geometry in its shallow regions (i.e., immediately below the ocean floor), which suggests that the

eastern part of the megasplay fault may have experienced long-term activity. The smooth and simply curved geometry of this zone indicates that current activity on this part of the fault may more readily transfer coseismic slip from the deep and ruptured zone to the shallowest part of the fault than occurs to other zones with deformed geometries. In turn, this highlights that thrusts with a smooth and thickened geometry at shallow depths may pose a higher risk for generating future tsunamis if the stress environment and material properties along the fault are maintained. Faults with such three-dimensional geometries at subduction margins should thus be identified and monitored in order to mitigate coastal damage that might result from future tsunamis.

[20] **Acknowledgments.** This research used data provided by the Integrated Ocean Drilling Program (IODP). Funding for this research was provided by Grants-in-Aid, for Scientific Research (KAKENHI: 213101115 and 24540489) and for Scientific Research on Innovative Areas (21107002). An earlier version of this manuscript was greatly improved after comments from G. Kimura and J.–O. Park. The authors also acknowledge the constructive comments of two anonymous reviewers and the editorial assistance of A. Newman.

[21] The Editor thanks two anonymous reviewers for their assistance in evaluating this paper.

References

Ammon, C. J., H. Kanamori, T. Lay, and A. A. Velasco (2006), The 17 July 2006 Java tsunami earthquake, *Geophy. Res. Lett.*, *33*, L24308, doi:10.1029/2006GL028005.

Bangs, N. L. B., G. F. Moore, S. P. S. Gulick, E. M. Pangborn, H. J. Tobin, S. Kuramoto, and A. Taira (2009), Broad, weak regions of the Nankai megathrust and implications for shallow coseismic slip, *Earth Planet Sci. Lett.*, *284*, 44–49.

Bardet, J.-P., C. E. Synolakis, H. L. Davies, F. Imamura, and E. A. Okal (2003), Landslide tsunamis: Recent findings and research directions, *Pure Appl Geophys.*, *160*, 1793–1809.

Cartwright, J. A., B. D. Trudgill, and C. S. Mansfield (1995), Fault growth by segment linkage: An explanation for scatter in maximum displacement and trace length data from the Canyonlands Grabens of SE Utah, *J. Struct. Geol.*, *17*, 1319–1326.

Ellis, M., and W. Dunlap (1988), Displacement variation along thrust faults: Implications for the development of large faults, *J. Struct. Geol.*, *10*, 183–192.

Evans, J. P. (1990), Thickness-displacement relationships for fault zones, *J. Struct. Geol.*, *12*, 1061–1065.

Gulick, S. P. S., N. L. B. Bangs, G. F. Moore, J. Ashi, K. M. Martin, D. S. Sawyer, H. J. Tobin, S. Kuramoto, and A. Taira (2010), Rapid forearc basin uplift and megasplay fault development from 3D seismic images of Nankai Margin off Kii Peninsula, Japan, *Earth Planet Sci. Lett.*, *300*, 55–62.

Hull, J. (1988), Thickness-displacement relationships for deformation zones, *J. Struct. Geol.*, *10*, 431–435.

Ito, Y., T. Tsuji, Y. Osada, M. Kido, D. Inazu, Y. Hayashi, H. Tsushima, R. Hino, and H. Fujimoto (2011), Frontal wedge deformation near the source region of the 2011 Tohoku-Oki earthquake, *Geophys. Res. Lett.*, *38*, L00G05, doi:10.1029/2011GL048355.

Kao, H., and W.-P. Chen (2000), The Chi-Chi earthquake sequence: Active out-of-sequence thrust faulting in Taiwan, *Science*, *288*, 2346–2349.

Kawamura, K., T. Sasaki, T. Kanamatsu, A. Sakaguchi, and Y. Ogawa (2012) Large submarine landslides in the Japan Trench: A new scenario for additional tsunami generation, *Geophys. Res. Lett.*, *39*, L05308, doi:10.1029/2011GL050661.

Kikuchi, M., M. Nakamura, and K. Yoshikawa (2003), Source rupture processes of the 1944 Tonankai earthquake and the 1945 Mikawa earthquake derived from low-gain seismograms, *Earth Planet Space*, *55*, 159–172.

Kimura, G., G. F. Moore, M. Strasser, E. Screaton, D. Curewitz, C. Streiff, and H. Tobin (2011), Spatial and temporal evolution of the megasplay fault in the Nankai Trough, *Geochem. Geophys. Geosyst.*, *12*, Q0A008, doi:10.1029/2010GC003335.

Kinoshita, M., H. Tobin, J. Ashi, G. Kimura, S. Lallement, E. J. Screaton, D. Curewitz, H. Masago, K. T. Moe, and the Expedition 314/315/316 Scientists (2009), *Proc. Integrated Ocean Drilling Program 314/315/316*, Integrated Ocean Drilling Program Management International, Inc, Washington, DC.

Matsumoto, T., and D. R. Tappin (2003), Possible coseismic large-scale landslide off the northern coast of Papua New Guinea in July 1998: Geophysical and geological results from SOS cruises, *Pure Appl. Geophys.*, *160*, 1923–1943.

Miyakawa, A., Y. Yamada, and T. Matsuoka (2010), Effect of increased shear stress along a plate boundary fault on the formation of an out-of-sequence thrust and a break in surface slope within an accretionary wedge, based on numerical simulations, *Tectonophysics*, *484*, 127–138.

Miyazaki, S., and K. Heki (2001), Crustal velocity field of southwest Japan: Subduction and arc-arc collision, *J. Geophys. Res.*, *106*, 4305–4326.

Moore, G. F., N. L. Bangs, A. Taira, S. Kuramoto, E. Pangborn, and H. Tobin (2007), Three-dimensional splay fault geometry and implications for tsunami generation, *Science*, *318*, 1128–1131.

Moore, G. F., et al. (2009), Structural and seismic stratigraphic framework of the NanTroSEIZE Stage 1 transect, in *Proc. Integrated Ocean Drilling Program, 314/315/316*, edited by M. Kinoshita et al., Integrated Ocean Drilling Program Management International, Inc, Washington, DC.

Morley, C. K. (1988), Out-of-Sequence Thrusts, *Tectonics*, *7*, 539–561.

Mukoyoshi, H., A. Sakaguchi, K. Otsuki, T. Hirono, and W. Soh (2006), Co-seismic frictional melting along an out-of-sequence thrust in the Shimanto accretionary complex. Implications on the tsunamigenic potential of splay faults in modern subduction zones, *Earth Planet Sci. Lett.*, *245*, 330–343.

Nieuwland, D. A., J. H. Leutscher, and J. Gast (2000), Wedge equilibrium in fold-and-thrust belts: Prediction of out-of-sequence thrusting based on sandbox experiments and natural examples, *Geol. Mijnbouw*, *79*, 81–91.

Park, J., T. Tsuru, S. Kodaira, A. Nakanishi, S. Miura, Y. Kaneda, Y. Kono, and N. Takahashi (2000), Out-of-sequence thrust faults developed in the coseismic slip zone of the 1946 Nankai Earthquake (Mw = 8.2) off Shikoku, southwest Japan, *Geophys. Res. Lett.*, *27*, 1033–1036.

Saffer, D., L. McNeill, T. Byrne, E. Araki, S. Toczko, N. Eguchi, K. Takahashi, and the Expedition 319 Scientists (2010), *Proc. Integrated Ocean Drilling Program*, 319 pp., Integrated Ocean Drilling Program Management International, Inc, Tokyo.

Sakaguchi, A., G. Kimura, M. Strasser, E. J. Screaton, D. Curewitz, and M. Murayama (2011), Episodic seafloor mud brecciation due to great subduction zone earthquakes, *Geology*, *39*, 919–922.

Satake, K. (2012), Tsunamis generated by submarine landslides, in *Submarine Mass Movements and Their Consequences: Advances in Natural and Technological Hazards Research*, vol. 31, edited by Y. Yamada et al., pp. 475–484, Springer, Netherlands.

Seno, T., S. Stein, and A. E. Gripp (1993), A model for the motion of the Philippine Sea Plate consistent with Nuvel-1 and geological data, *J. Geophys. Res.*, *98*, 17,941–17,948.

Sheriff, R. E. (2002), *Encyclopedic Dictionary of Applied Geophysics*, 4th ed., Geophysical References Series 13, Society of Exploration Geophysics, Tulsa, Oklahoma.

Strasser, M., et al. (2009), Origin and evolution of a splay fault in the Nankai accretionary wedge, *Nat. Geosci.*, *2*, 648–652.

Tobin, H. J., and M. Kinoshita (2006), NanTroSEIZE: The IDOP Nankai Trough seismogenic zone experiment, *Sci. Drill.*, *2*, 23–27.

Waldhauser, F., D. P. Schaff, T. Diehl, and E. R. Engdahl (2012), Splay faults imaged by fluid-driven aftershocks of the 2004 *Mw* 9.2 Sumatra-Andaman earthquake, *Geology*, *40*, 243–246.

Walsh, J. J., W. R. Bailey, C. Childs, A. Nicol, and C. G. Bonson (2003), Formation of segmented normal faults: A 3-D perspective, *J. Struct. Geol.*, *25*, 1251–1262.

Yamada, Y., K. Baba, and T. Matsuoka (2006), Analogue and numerical modelling of accretionary prisms with a decollement in sediments, in *Numerical and Analogue Modelling of Crustal-Scale Processes*, Geological Society Special Publication, vol. 253, edited by S. Buiter and G. Scherurs, pp. 169–183, Geological Society, London.

Yamada, Y., L. McNeill, J. C. Moore, and Y. Nakamura (2011), Structural styles across the Nankai accretionary prism revealed from LWD borehole images and their correlation with seismic profile and core data: Results from NanTroSEIZE Stage 1 expeditions, *Geochem. Geophys. Geosyst.*, *12*, Q0AD15, doi:10.1029/2010GC003365.